Supporting Information

Total OH reactivity of emissions from humans: in-situ measurement and budget analysis

Nijing Wang[1*], *Nora Zannoni*[1], *Lisa Ernle*[1], *Gabriel Bekö*[2], *Pawel Wargocki*[2], *Mengze Li*[1], *Charles J. Weschler*[2, 3], *Jonathan Williams*[1, 4]

[1]Max Planck Institute for Chemistry, Mainz, Germany

[2]International Centre for Indoor Environment and Energy, Department of Civil Engineering, Technical University of Denmark, Lyngby, Denmark

[3]Environmental and Occupational Health Sciences Institute, Rutgers University, New Jersey, United States

[4]The Cyprus Institute, Nicosia, Cyprus

*corresponding author: nijing.wang@mpic.de

Pages: S1 – S23
Tables: S1, S2, S3, S4
Figures: S1, S2

Comparative reactivity method (CRM) operating procedures

The reference molecule used in CRM is pyrrole (C_4H_5N)[1], which reacts with OH radicals at comparable rates with reactive species and is not commonly presented in the measured air. Pyrrole can be sensitively detected by PTR-MS due to its higher proton affinity than water. For CRM, three measurement modes were implemented to quantify the total OH reactivity: (1) pyrrole together with an OH radical scavenger[2] was introduced to define the initial pyrrole level (C1 mode); (2) the OH radical scavenger was stopped and the level of pyrrole after reaction with OH radicals was recorded (C2 mode); (3) finally sample air from the chamber was introduced into the reactor with the pyrrole, the resulting competition for the available OH leading to a third pyrrole level (C3 mode). Based on these three modes, the total reactivity (R, s^{-1}) was calculated using the following equation:

$$R = \frac{(C3 - C2)}{(C1 - C3)} \cdot C1 \cdot k_{Pyrrol + OH} \qquad \text{Eq. (1)}$$

where $C1$, $C2$ and $C3$ refer to previously mentioned pyrrole concentrations (molecules cm^{-3}) in the corresponding mode and $k_{Pyrrol + OH}$ refers to the rate constant of pyrrole reacting with OH radicals[3]. During an experiment, the OH reactivity measurement was switched between C2 mode and C3 mode every 5 minutes, and the C1 mode was usually measured at the end of the day. The pyrrole level measured by PTR-QMS was calibrated frequently using a gas standard (Westfalen AG, Germany).

Interference and corrections of OH reactivity data analysis

- **Pyrrole photolysis**

The pen ray mercury lamp used for water photolysis would also lead to pyrrole photolysis, which would complicate the system[1]. Therefore, the initial pyrrole level (C1) was determined when the lamp was on, which already considered the loss of pyrrole due to photolysis.

- **Humidity correction**

As the OH radical concentration is dependent on the water vapor inside the reactor, any difference in humidity between the C2 and C3 modes must also be taken into account. The humidity correction was done by humidifying the air flow of CRM at different degrees under C2 mode[1]. The humidity was monitored by the ratio of *m/z* 37 (water cluster) and *m/z*19 (primary ions). Then a correction factor can be derived from the slope of humidity vs. C2 pyrrole level, with an error of 29%. The correction factor was then applied to the C2 level during measurements to correct the humidity difference between C2 mode and C3 mode. The correction of the C2 level was on average 0.06 ± 0.04 ppb, leading to a reactivity of 0.4 ± 0.2 s^{-1}.

- **Correction factor for not being at pseudo-first-order conditions**

Equation (1), used to derive the OH reactivity, is based on the assumption of pseudo-first-order conditions. These conditions cannot be entirely fulfilled under normal operating conditions when maintaining a reasonable sensitivity. Therefore, a correction factor was applied as a function of the pyrrole/OH ratios. The method used to derive the correction factor is based on Michoud, et al. [4]. The correction factor was obtained from injecting known amount of a standard gas under different pyrrole/OH ratios conditions. A factor can be obtained from measured reactivity vs. calculated reactivity for that gas. Total of five standard gases with different rate constants reacting with the

OH radical including propane, propene, isoprene, α-pinene and acetaldehyde were tested within the pyrrole/OH range observed during the entire campaign. A linear fit was applied among all the factors derived from the tests, resulting in a linear relationship between the correction factor and pyrrole/OH ratio (f = a[pyrrole/OH]+b), with an error of 31%. Throughout the campaign, the pyrrole/OH ratio ranged from 2.0 - 3.0, which increased the OH reactivity by a factor of 1.3 to 2.7.

- **NO_x interference**

Previous studies have also shown that NO_x can potentially cause an interference to CRM measurements by producing OH radicals via reactions with HO_2 radicals. Relevant corrections should be applied if the measured conditions have abundant NO_x (NO > 10ppb[1]) and it should be noted that NO has a more significant interference compared to NO_2 at the same level[4-6]. NO and NO_2 were continuously monitored by a chemiluminescence NO/NO_x analyzer (ECO PHYSICS, model CLD 700 AL). The mixing ratios of NO and NO_2 in the occupied chamber were near or below the detection limit (1 ppb) for most of the time during the entire experimental period. By taking into account the dilution factor of the CRM (1.37), NO and NO_2 levels in the glass reactor would be lower than the detection limit most of the time. Therefore, NO_x interference to the CRM could be neglected and no correction was applied. NO and NO_2 have OH rate constants comparable to some VOCs shown in Table S1 (9.70×10^{-12} cm^3 $molecules^{-1}$ s^{-1} and 9.80×10^{-12} cm^3 $molecules^{-1}$ s^{-1} for NO and NO_2, respectively[7]). The upper limit of the NO_x contribution to the total reactivity (assuming 2 ppb of NO or NO_2) would be 0.5 s^{-1} (3.0% of the total reactivity under ozone-free condition and 1.5% under ozone-present condition). This is comparable to some top ten OH reactivity contributing species (Table 2). The NOx data were mostly at or below the detection limit and no clear trend can be observed due to human occupancy; the 2 ppb of NOx assumption represents an upper limit estimate rather than a measurement. Therefore, NOx was not included in the calculation of OH reactivity in the study.

- **Ozone interference**

High level of ozone was also found to cause interference depending on the CRM system[5]. For ozone interference test, different levels of ozone (0 -110 ppb) was introduced to the empty chamber. The measured OH reactivity interference due to ozone was less than 3 s^{-1} at the highest ozone level, which is lower than the limit of detection for CRM during this campaign (5 s^{-1}). The ozone level in the chamber during the afternoon steady state when occupied was around 37 ppb, resulting in 1 s^{-1} difference in the measured reactivity which was much smaller than the total uncertainty of the measured reactivity (16 – 22 s^{-1}). As the ozone interference is negligible and extra uncertainty would be introduced from the correction factor, no correction was applied.

Calculations of precision and total uncertainty of CRM

When a test gas is injected into the CRM at several known concentrations, the corresponding mean reactivity at each concentration can be obtained together with the standard deviation. By plotting the relative reactivity (standard deviation/mean reactivity, $R_{relative}$) against the mean reactivity ($R_{measured}$), an exponential curve is obtained that can be fit with the equation:

$$R_{relative} = a + b * \exp\,(c * R_{measured})$$

where parameters a, b and c are derived from curve fitting and the relative reactivity defines the precision. For this study, results from test gases mentioned in “Correction factor for not being at pseudo-first-order conditions” were included to derive the fitting results. Based on the measured reactivity of real measurements, the precision can be calculated by applying this equation to each data point.

The accuracy of the CRM is the propagation of uncertainties from the pyrrole standard gas concentration, the dilution factors derived from flow measurements, the OH rate constant of pyrrole, the humidity correction, and the non-pseudo-first-order correction. Detailed numbers can be found in Table S1.

Table S1 Uncertainties in the CRM

Uncertainties from	**Uncertainties (%)**
Pyrrole standard gas	10
Dilution factors	0.16
OH rate constant of pyrrole	14
Humidity correction	29
Non-pseudo-first-order correction	31
Propagated accuracy	46
Total uncertainty (mean and median)	50

Empty-chamber background

The background obtained from the empty chamber before volunteers entered was in general very stable for calculated reactivity (3 s^{-1} on average with a variability of 10%). For measured total reactivity, the background was typically around or under the detection limit (5 s^{-1}).

Definition of steady-state condition

As the calculated reactivity has less uncertainty than measured reactivity, the steady-state condition was verified by the relative change of calculated reactivity during the 15 minutes before volunteers exited the chamber. This is to avoid any effect left due to requested movements by the volunteers (standing up and stretching) every hour during each experimental period. For all the experiments, the relative changes ((max-min)/mean) were below 5% (0.8-5.0%, mean 2.1%), which is much less than the uncertainty of the calculated OH reactivity (21% - 45%, median and mean 29%). Therefore, the time period of 15 minutes is suitable to be considered as steady-state condition.

Adjustment method applied for OH reactivity per person comparison

To be able to compare the OH reactivity per person ($s^{-1}p^{-1}$) in the ICHEAR chamber experiments with other studies, the OH reactivity per person obtained from other studies were adjusted for the room volume and the air change rate (ACR) applied in the ICHEAR chamber experiments using the following equations:

$$RP_a = \frac{Room\ volume\ (other\ studies)}{22.5\ m^3} \times \frac{ACR\ (other\ studies)}{3.2\ h^{-1}} \times RP_b$$

where RP_a refers to the OH reactivity per person after the adjustment and RP_b refers to the OH reactivity per person before the adjustment, which is obtained from the total OH reactivity divided by the number of occupants in that environment. 22.5 m^3 is the ICHEAR chamber volume and 3.2 h^{-1} is the ACR for the chamber. The per-person OH reactivity before the adjustment (RP_b) for the other studies mentioned in Table 3 were estimated using reported values. For the museum gallery room study[70], RP_b is derived from the incremental total OH reactivity (14 s^{-1}) during the high occupancy event (compared to the low occupancy condition) divided by the number of occupants (176 on average). For the classroom study[71] and cinema study[72], the RP_b was calculated based on the VOC emission rates (μg $h^{-1}p^{-1}$) reported in each work. As both studies used PTR-ToF-MS, some masses could only be assigned to chemical formulas instead of specific compounds. Therefore, we only included masses with specific compound assignments reported in those two studies to calculate the total OH reactivity per person. Those included VOCs were mostly measured during the present experiments as well. The emission rates were first converted to mixing ratios per person (ppb p^{-1}) based on the indoor space volume and the ACR reported in each study. Then the total OH reactivity per person was calculated using Eq.1 in the main text. The estimated RP_b of those two studies may slightly underestimate the actual values as those masses without a specific compound assignment (accounting for < 20% of the total VOC emission rates) were not included in the calculation.

Potential artifacts from decomposition of hydroperoxides

It has been reported that metal surface can act as a catalyst for the decomposition of organic hydroperoxides, and that this is temperature dependent.[73] It has been further reported that with stainless tubing, the conversion rates for ISOPOOH to formaldehyde at room temperature were not significant (below 10%) but increased to 50% at 160 °C[73]. As the temperature in the ICHEAR chamber study was always less than ~ 31°C, this artifact on the stainless-steel chamber walls is not anticipated to be important. However, for the PTR-ToF-MS instrument, this interference may still exist as the drift tube was heated to 60 °C, converting a small amount of ISOPOOH to other products. Another important factor to consider is that in the ICHEAR chamber study, the main oxidant was ozone instead of OH radicals (which are the major oxidant outdoors). MVK and MACR, rather than ISOPOOH, are the major products of isoprene ozonolysis[74]. Furthermore, the reaction between ozone and isoprene is relatively slow (1.1×10^{-3} ppb/h at 298 K)[7]; at the average ozone concentration (37 ppb) used in ICHEAR, the O_3/isoprene reaction occurs at a rate ($0.04\ h^{-1}$) substantially slower than the air change rate ($3.2\ h^{-1}$). Hence, production of ISOPOOH via ozone reaction was quite small in ICHEAR. The formation of ISOPOOH, to the extent that it occurred in ICHEAR, was probably from isoprene/OH oxidation as OH radicals can be generated during the ozonolysis of unsaturated compounds. Assuming the extreme scenario that measured MVK/MACR were half decomposed from ISOPOOH, it would increase the calculated reactivity during ozone-present condition by $0.6\ s^{-1}$ as ISOPOOH has a faster reaction rate constant compared to MVK/MACR ($9.65 \times 10^{-11}\ cm^3\ molecules^{-1}\ s^{-1}$, averaged of (1,2)-ISOPOOH and (4,3)-ISOPOOH)[75]. The calculated increase of $0.6\ s^{-1}$ is within the standard deviation of the total calculated reactivity

(1.4 s^{-1}). Therefore, we judge that the interference should be small. In terms of reactivity measurement, as the PTR-QMS measured the air coming out of the glass reactor and temperature inside the reactor was around 35-40 °C, there should be no interference.

Table S2. List of compounds used in calculating the estimated OH reactivity.

Compound group	Protonated *m/z* from PTR-MS	Formula assignment	Possible compound assignment	k_{Xi+OH} (cm^3 $molecules^{-1}$ s^{-1}) at 298K*	Remarks**	Reference
Hydrocarbons (HC)		C5H8	isoprene	1.00 × 10^{-10}	Data from fast-GC	7 (IUPAC)
	79.053	C6H6	benzene	1.20 × 10^{-12}	PTR calibrated	7 (IUPAC)
	93.070	C7H8	toluene	5.60 × 10^{-12}	PTR calibrated	7 (IUPAC)
	105.070	C8H8	styrene	5.80 × 10^{-11}		8
	107.086	C8H10	xylene	1.70 × 10^{-11} (1.36 -2.31) × 10^{-11}	PTR calibrated; k rate averaged from listed isomeric compounds	8
	119.086	C9H10	2-phenylpropene	5.30 × 10^{-11}		9
	121.101	C9H12	trimethylbenzene	4.06 × 10^{-11} (3.25 -5.67) × 10^{-11}	PTR calibrated; k rate averaged from listed isomeric compounds	8
	133.101	C10H12	benzene,(2-methyl-1-propenyl)-	3.30 × 10^{-11}		9
	137.132	C10H16	monoterpenes	1.64 × 10^{-10}	PTR calibrated using α-pinene; k rate of limonene was taken	7 (IUPAC)
OVOC Alcohols	33.034	CH4O	methanol	9.00 × 10^{-13}	PTR calibrated	7 (IUPAC)
	47.049	C2H6O	ethanol	3.20 × 10^{-12}		7 (IUPAC)
OVOC Acids	43.018 61.029	C2H4O2	acetic acid	8.00 × 10^{-13}		10
	73.029	C3H4O2	acrylic acid	1.75 × 10^{-11}		11
	89.023	C3H4O3	pyruvic acid	1.24 × 10^{-13}		12
OVOC Aromatics	95.049	C6H6O	phenol	3.27 × 10^{-11}		13
	107.049	C7H6O	benzaldehyde	1.20 × 10^{-11}		7 (IUPAC)
	109.029	C6H4O2	1,4-benzoquinone	4.60 × 10^{-12}		14
	109.065	C7H8O	methylphenol/methoxybenzene/toluene-1,2-oxide 3/2-methyloxepin	7.74 × 10^{-11} (2.54 -21.0) × 10^{-11}	k rate averaged from listed isomeric compounds	15-17

OVOC Aromatics	121.065	C8H8O	tolualdehyde	1.60×10^{-11}		8
	123.044	C7H6O2	p-benzoquinone, 2-methyl-	2.35×10^{-11}		14
	123.081	C8H10O	dimethylphenol	8.48×10^{-11}		16
	125.060	C7H8O2	4-methoxyphenol /3-methoxyphenol/2-methoxyphenol	8.94×10^{-11} $(7.44\text{-}9.80) \times 10^{-11}$	k rate averaged from listed isomeric compounds	16
	135.081	C9H10O	dimethylbenzaldehyde	2.74×10^{-11} $(2.46\text{-}3.70) \times 10^{-11}$	k rate averaged from listed isomeric compounds	18
	137.060	C8H8O2	1,4-benzodioxane	2.52×10^{-11}		19
	149.096	C10H12O	2,4,5-trimethylbenzaldehyde	4.27×10^{-11}		20
OVOC Carbonyls	31.018	CH2O	formaldehyde	9.37×10^{-12}		8
	45.033	C2H4O	acetaldehyde	1.50×10^{-11}	PTR calibrated	7 (IUPAC)
	57.034	C3H4O	acrolein	2.00×10^{-11}		21
	59.048	C3H6O	acetone	1.80×10^{-13}	PTR calibrated	7 (IUPAC)
	71.048	C4H6O	methyl vinyl ketone (MVK)/methacrolein (MACR)/isoprene hydroxy hydroperoxide (ISOPOOH)	2.45×10^{-11} $(2.0\text{ -}2.9) \times 10^{-11}$	PTR calibrated; k rate averaged from MVK and MACR	7 (IUPAC)
	73.064	C4H8O	methyl ethyl ketone	1.10×10^{-12}	PTR calibrated	7 (IUPAC)
	75.044	C3H6O2	hydroxyacetone	3.00×10^{-12}		22
	83.049	C5H6O	4-oxopentanal fragment; methylfuran	2.00×10^{-11}	k rate of 4OPA was taken	23
	85.028	C4H4O2	butenedial	5.21×10^{-11}		24
	85.065	C5H8O	2-pentenal	4.37×10^{-11}		25
	87.044	C4H6O2	1,4-butanedial	5.70×10^{-11}	k rate of 4-hydroxy-2-butenal was taken	26
	87.081	C5H10O	pentanal	2.80×10^{-11}		8
	97.020	C5H4O2	2 or 3-furancarboxaldehyde	4.18×10^{-11} $(3.50\text{-}4.85) \times 10^{-11}$	k rate averaged from listed isomeric compounds	27
	97.065	C6H8O	2,4-hexadienal	5.90×10^{-11}		28
	99.045	C5H6O2	4-oxo-2-pentenal	5.58×10^{-11}		24

OVOC Carbonyls	99.081	C6H10O	cis-3-hexenal; (2e)-2-hexenal; 2-pentenal, 2-methyl-	4.64×10^{-11} $(3.93 - 6.60) \times 10^{-11}$	k rate averaged from listed isomeric compounds	29-31
	101.060	C5H8O2	4-oxopentanal (4-OPA)	2.00×10^{-11}		23
	101.096	C6H12O	hexanal	3.00×10^{-11}		8
	103.075	C5H10O2	1-hydroxy-2-methyl-3-butanone	1.62×10^{-11}		32
	109.101 127.112	C8H14O	6-methyl-5-hepten-2-one (6-MHO)	1.57×10^{-10}		33
	111.081	C7H10O	4-methylenehex-5-enal/(3z)-4-methylhexa-3,5-dienal/(3e)-4-methylhexa-3,5-dienal/4-methylcyclohex-3-en-1-one	1.69×10^{-10} $(1.10 - 3.10) \times 10^{-10}$	k rate averaged from listed isomeric compounds	34
	113.096	C7H12O	(e)-2-hepten-1-al	4.39×10^{-11}		25
	115.112	C7H14O	2, 3-dimethylpentanal; heptanal	3.20×10^{-11} $(2.96 - 4.20) \times 10^{-11}$	k rate averaged from listed isomeric compounds	35, 36
	127.076	C7H10O2	3-methyl-3-hexene-2,5-dione	9.40×10^{-11}		20
	129.127	C8H16O	octanal	3.00×10^{-11}	k rate estimated, same as hexanal	
	139.112	C9H14O	bicyclo[2.2.1]heptan-2-one,3,3-dimethyl-/sabinaketone/ bicyclo[3.1.1]heptan-2-one, 6,6-dimethyl-	8.85×10^{-12} $(5.15 - 14.3) \times 10^{-12}$	k rate averaged from listed isomeric compounds	37, 38
	123.117 141.127	C9H16O	trans-2-nonenal	4.35×10^{-11}		30
	125.132 143.143	C9H18O	nonanal	3.60×10^{-11}		39
	153.127	C10H16O	camphor	3.80×10^{-12}		40
	155.154	C10H18O	geraniol; citronellal	1.90×10^{-10} $(1.50 - 2.31) \times 10^{-10}$	k rate averaged from listed isomeric compounds	41, 42

OVOC Carbonyls	137.097 155.107	C9H14O2	4-methyl-4-octene-1,8-dial (4-MOD)	1.57×10^{-10}	k rate estimated, same as 6-MHO	
	139.148 157.159	C10H20O	C10 aliphatic carbonyls (decanal)	3.60×10^{-11}	k rate estimated, same as nonanal	
	151.112 169.123	C10H16O2	4-methyl-8-oxo-noennal (4-MON)	1.57×10^{-10}	k rate estimated, same as 6-MHO	
	171.175	C11H22O	C11 aliphatic carbonyls (undecanal)	3.60×10^{-11}	k rate estimated, same as nonanal	
	177.164 195.175	C13H22O	geranyl acetone	1.57×10^{-10}	k rate estimated, same as 6-MHO	
		C3H6O	propanal	2.00×10^{-11}	Data from fast-GC	7 (IUPAC)
OVOC others	69.034	C4H4O	furan	4.04×10^{-11}		43
	89.060	C4H8O2	acetic acid, ethyl ester; formic acid, 1-methylethyl ester	2.04×10^{-12} $(1.69 - 2.4) \times 10^{-12}$	k rate averaged from listed isomeric compounds	44, 45
	111.044	C6H6O2	aromatic phenol/e,z- and e,e-2,4-hexadienedial/2-furancarbocaldehyde, 5-methyl-/1,2-dihydroxybenzene/1,4-benzenediol/1,3-benzenediol	5.19×10^{-11} $(0.44 - 10.3) \times 10^{-11}$	k rate averaged from listed isomeric compounds	14, 46, 47
	113.060	C5H10O2	formic acid, tert-butyl ester/butanoic acid, methyl ester/formic acid, butyl ester/propanoic acid, 2-methyl-, methyl ester/	2.63×10^{-12} $(0.68 - 3.82) \times 10^{-12}$	k rate averaged from listed isomeric compounds	48-52
	115.075	C6H10O2	ethyl crotonate/3-methyl-2,4-pentanedione/2,5-hexanedione/methacrylic acid ethyl ester	3.25×10^{-11} $(0.67 - 4.96) \times 10^{-11}$	k rate averaged from listed isomeric compounds	53-56

OVOC others	117.091	C6H12O2	butanoic acid, 2-methyl-, methyl ester/methyl valerate/acetic acid, butyl ester/isobutyl acetate/propanoic acid, propyl ester/butanoic acid, ethyl ester	4.17×10^{-12} $(0.56 - 6.33) \times 10^{-12}$	k rate averaged from listed isomeric compounds	48, 49, 52, 57-59
	129.091	C7H12O2	n-butyl acrylate/4-pentenyl acetate	3.28×10^{-11} $(2.28 - 4.33) \times 10^{-11}$	k rate averaged from listed isomeric compounds	60, 61
	143.107	C8H14O2	1-hydroxy-6-methyl-5-hepten-2-one (OH-6MHO)	6.60×10^{-11}	k rate of butyl methacrylate was taken	60
Nitrogen containing	42.033	C2H3N	acetonitrile	2.20×10^{-14}	PTR calibrated	7 (IUPAC)
		NH3	ammonia	1.57×10^{-13}	Data from Picarro	7 (IUPAC)
	46.029	CH3NO	formamide/formaldoxime	2.97×10^{-12} $(1.50 - 4.44) \times 10^{-12}$	k rate averaged from listed isomeric compounds	62, 63
	70.065	C4H7N	butyronitrile	2.56×10^{-13}		64
	74.024	C2H3NO2	nitroethene	1.20×10^{-12}		65
Sulfur containing	49.011	CH4S	methanethiol	3.30×10^{-11}		7 (IUPAC)
	63.026	C2H6S	dimethyl sulfide	4.80×10^{-12}	PTR calibrated	7 (IUPAC)
	91.057	C4H10S	tert-butylthiol; 2-butanethiol; 1-propanethiol, 2-methyl-; 1-butanethiol;	4.22×10^{-11} $(2.91 - 5.60) \times 10^{-11}$	k rate averaged from listed isomeric compounds	66
	95.016	C2H6O2S	dimethyl sulfone	3.00×10^{-13}		67

IUPAC: preferred values recommend by IUPAC were taken.

* rate constant ranges listed in parentheses refer to the range of rate constants of listed isomeric compounds.

**Compounds without mentioning as "PTR calibrated", "fast-GC" nor "Piccaro" refer to the mixing ratios of species measured by PTR-ToF-MS were calculated based on theoretic method using a constant rate coefficient (2.0E-9 cm^3s^{-1}) for the reactions with H_3O^+ [68], except for 6-MHO where a known rate coefficient (3.8E-9 cm^3s^{-1}) was used [69].

Table S3. Top ten species contributing to the calculated OH reactivity of breath emissions (Experiment 12, adult group A3) under ozone-free and ozone-present conditions.

	Mass (H^+)	Compounds	OH Reactivity (s^{-1})	Fraction
Ozone-free	*	isoprene	11.9	95.3%
	33.034	methanol	0.15	1.2%
	137.132	limonene	0.09	0.7%
	59.048	acetone	0.08	0.6%
	69.034	furan	0.04	0.3%
	61.029	acetic acid	0.04	0.3%
	87.044	1,4-butanedial	0.03	0.2%
	127.112	6MHO	0.02	0.2%
	91.057	C4H10S	0.02	0.2%
	63.026	DMS	0.01	0.1%
		Sum of top 10 species	**12.3**	**99.1%**
		Sum of all species	**12.5**	
Ozone-present	*	isoprene	11.2	82.5%
	87.044	1,4-butanedial	0.5	3.4%
	101.096	4OPA	0.3	2.0%
	45.034	acetaldehyde	0.2	1.5%
	127.112	6MHO	0.1	0.9%
	*	propanal	0.1	0.9%
	71.049	C4H6O	0.1	0.8%
	33.034	methanol	0.1	0.8%
	69.034	furan	0.1	0.7%
	61.029	acetic acid	0.1	0.7%
		Sum of top 10 species	**12.8**	**94.3%**
		Sum of all species	**13.5**	

*isoprene and propanal data were obtained from fast-GC

Table S4. Top ten species contributing to the calculated OH reactivity of dermal emissions (Experiment 13, adult group A3) under ozone-free and ozone-present conditions.

	Mass (H^+)	Compounds	OH Reactivity (s^{-1})	Fraction
Ozone-free	45.034	acetaldehyde	0.7	15.1%
	69.070	isoprene	0.3	7.2%
	127.112	6MHO	0.3	7.0%
	95.049	phenol	0.3	6.6%
	137.133	limonene	0.3	6.3%
	#	ammonia	0.2	4.6%
	121.065	tolualdehyde	0.2	4.5%
	91.057	C4H10S	0.2	4.3%
	87.044	1,4-butanedial	0.2	4.1%
	71.049	C4H6O	0.2	3.8%
		Sum of top 10 species	**2.9**	**63.4%**
		Sum of all species	**4.6**	
Ozone-present	127.112	6MHO	13.2	41.8%
	101.096	4OPA	3.6	11.3%
	87.044	1,4-butanedial	1.5	4.6%
	45.034	acetaldehyde	1.3	4.1%
	157.159	decanal	0.7	2.3%
	143.143	nonanal	0.7	2.3%
	141.127	nonenal	0.7	2.2%
	143.107	OH-6MHO	0.7	2.2%
	137.133	limonene	0.6	2.0%
	195.186	geranal acetone	0.5	1.7%
		Sum of top 10 species	**23.5**	**74.5%**
		Sum of all species	**31.5**	

#ammonia data was from Picarro.

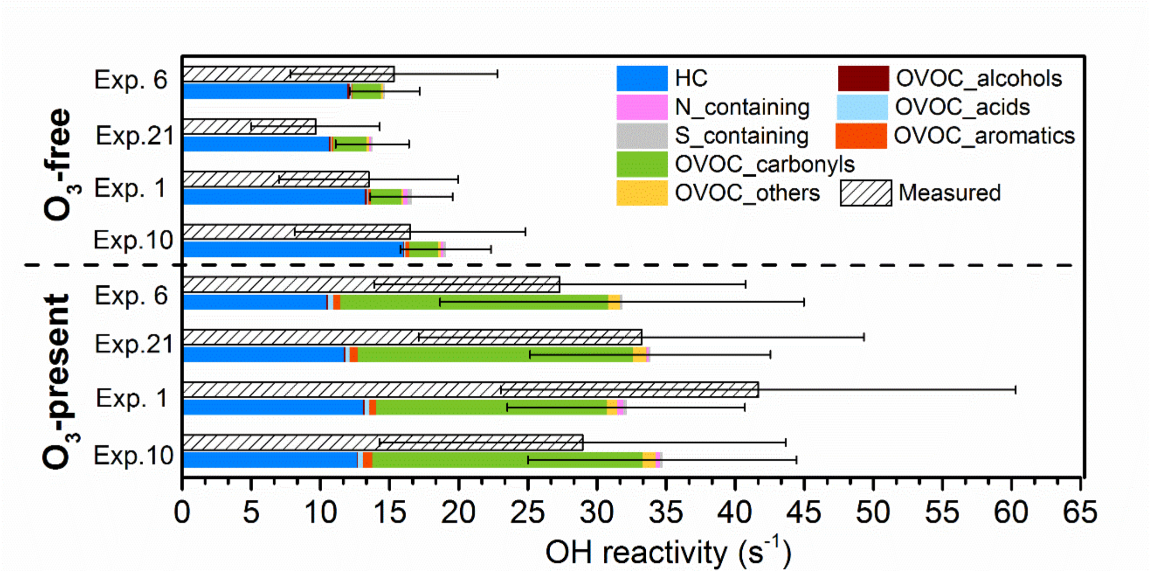

Figure S1. Calculated and measured OH reactivity during ozone-free and ozone-present steady-state conditions of the benchmark experiments with young adults. Error bars represent the total uncertainty of measured OH reactivity and calculated OH reactivity. Experiment 21 is a replicate of Experiment 6.

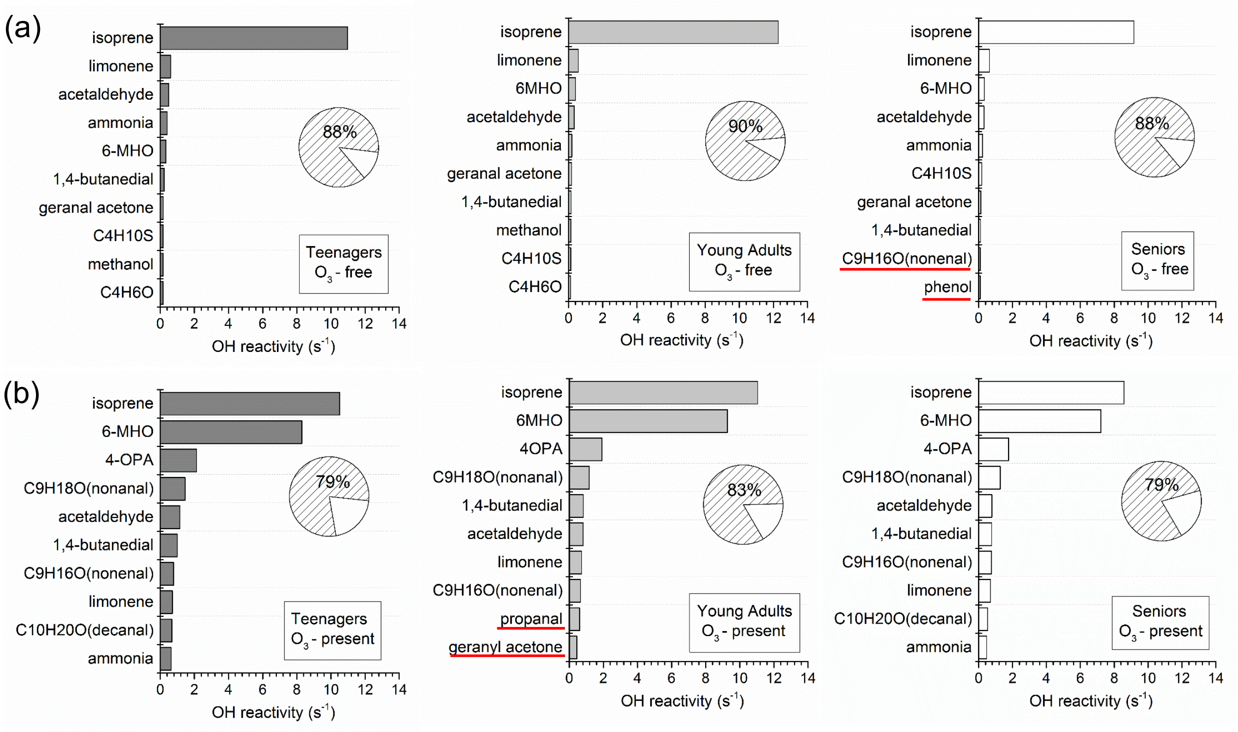

Figure S2. Top ten species contributing to the total OH reactivity for teenagers, young adults and seniors under (a) ozone-free condition and (b) ozone-present condition. The species marked with red underline represent unique species that do not appear among the top ten species of the other two groups. The pie chart in each plot represents the fractions of the total reactivity attributable to the top ten species (hatched) and remaining species (blank).

References

1. Sinha, V.; Williams, J.; Crowley, J.; Lelieveld, J., The Comparative Reactivity Method–a new tool to measure total OH Reactivity in ambient air. *Atmospheric Chemistry and Physics* **2008,** *8*, (8), 2213-2227.
2. Zannoni, N.; Dusanter, S.; Gros, V.; Sarda Esteve, R.; Michoud, V.; Sinha, V.; Locoge, N.; Bonsang, B., Intercomparison of two comparative reactivity method instruments inf the Mediterranean basin during summer 2013. *Atmospheric Measurement Techniques* **2015,** *8*, (9), 3851-3865.
3. Dillon, T. J.; Tucceri, M. E.; Dulitz, K.; Horowitz, A.; Vereecken, L.; Crowley, J. N., Reaction of Hydroxyl Radicals with C4H5N (Pyrrole): Temperature and Pressure Dependent Rate Coefficients. *The Journal of Physical Chemistry A* **2012,** *116*, (24), 6051-6058.
4. Michoud, V.; Hansen, R. F.; Locoge, N.; Stevens, P. S.; Dusanter, S., Detailed characterizations of the new Mines Douai comparative reactivity method instrument via laboratory experiments and modeling. *Atmospheric Measurement Techniques* **2015,** *8*, (8), 3537-3553.
5. Fuchs, H.; Novelli, A.; Rolletter, M.; Hofzumahaus, A.; Pfannerstill, E. Y.; Kessel, S.; Edtbauer, A.; Williams, J.; Michoud, V.; Dusanter, S.; Locoge, N.; Zannoni, N.; Gros, V.; Truong, F.; Sarda-Esteve, R.; Cryer, D. R.; Brumby, C. A.; Whalley, L. K.; Stone, D.; Seakins, P. W.; Heard, D. E.; Schoemaecker, C.; Blocquet, M.; Coudert, S.; Batut, S.; Fittschen, C.; Thames, A. B.; Brune, W. H.; Ernest, C.; Harder, H.; Muller, J. B. A.; Elste, T.; Kubistin, D.; Andres, S.; Bohn, B.; Hohaus, T.; Holland, F.; Li, X.; Rohrer, F.; Kiendler-Scharr, A.; Tillmann, R.; Wegener, R.; Yu, Z.; Zou, Q.; Wahner, A., Comparison of OH reactivity measurements in the atmospheric simulation chamber SAPHIR. *Atmospheric Measurement Techniques* **2017,** *10*, (10), 4023-4053.
6. Pfannerstill, E. Y.; Wang, N.; Edtbauer, A.; Bourtsoukidis, E.; Crowley, J. N.; Dienhart, D.; Eger, P. G.; Ernle, L.; Fischer, H.; Hottmann, B.; Paris, J.-D.; Stönner, C.; Tadic, I.; Walter, D.; Lelieveld, J.; Williams, J., Shipborne measurements of total OH reactivity around the Arabian Peninsula and its role in ozone chemistry. *Atmospheric Chemistry and Physics* **2019,** *19*, (17), 11501-11523.
7. IUPAC Task Group on Atmospheric Chemical Kinetic Data Evaluation: Datasheets - gas phase: http://iupac.pole-ether.fr/
8. Atkinson, R.; Arey, J., Atmospheric Degradation of Volatile Organic Compounds. *Chemical Reviews* **2003,** *103*, (12), 4605-4638.
9. Chiorboli, C.; Maldotti, A.; Bignozzian, C.; Carassitik, V. Atmospheric photochemistry: kinetics and mechanism of reactions between aromatic olefins and hydroxyl radical, *Proceedings of the Second European Symposium on Physico-Chemical Behaviour of Atmospheric Pollutants (conference)*, ***1981***, pp 228-233.
10. Atkinson, R.; Baulch, D.; Cox, R.; Crowley, J.; Hampson Jr, R.; Kerr, J.; Rossi, M.; Troe, J., Summary of evaluated kinetic and photochemical data for atmospheric chemistry. *IUPAC Subcommittee on gas kinetic data evaluation for atmospheric chemistry* **2001,** *20*.
11. Teruel, M. A.; Blanco, M. B.; Luque, G. R., Atmospheric fate of acrylic acid and acrylonitrile: rate constants with Cl atoms and OH radicals in the gas phase. *Atmospheric Environment* **2007,** *41*, (27), 5769-5777.
12. Mellouki, A.; Mu, Y., On the atmospheric degradation of pyruvic acid in the gas phase. *Journal of Photochemistry and Photobiology A: Chemistry* **2003,** *157*, (2-3), 295-300.
13. Sørensen, M.; Hurley, M.; Wallington, T.; Dibble, T.; Nielsen, O., Do aerosols act as catalysts in the OH radical initiated atmospheric oxidation of volatile organic compounds? *Atmospheric Environment* **2002,** *36*, (39-40), 5947-5952.

14. Olariu, R. I.; Barnes, I.; Becker, K. H.; Klotz, B., Rate coefficients for the gas-phase reaction of OH radicals with selected dihydroxybenzenes and benzoquinones. *International Journal of Chemical Kinetics* **2000,** *32*, (11), 696-702.

15. Coeur-Tourneur, C.; Henry, F.; Janquin, M.-A.; Brutier, L., Gas-phase reaction of hydroxyl radicals with m-, o- and p-cresol. *International Journal of Chemical Kinetics* **2006,** *38*, (9), 553-562.

16. Coeur-Tourneur, C.; Cassez, A.; Wenger, J. C., Rate Coefficients for the Gas-Phase Reaction of Hydroxyl Radicals with 2-Methoxyphenol (Guaiacol) and Related Compounds. *The Journal of Physical Chemistry A* **2010,** *114*, (43), 11645-11650.

17. Klotz, B.; Barnes, I.; Golding, B. T.; Becker, K.-H., Atmospheric chemistry of toluene-1,2-oxide/2-methyloxepin. *Physical Chemistry Chemical Physics* **2000,** *2*, (2), 227-235.

18. Clifford, G. M.; Wenger, J. C., Rate coefficients for the gas-phase reaction of hydroxyl radicals with the dimethylbenzaldehydes. *International journal of chemical kinetics* **2006,** *38*, (9), 563-569.

19. Atkinson, R.; Arey, J.; Tuazon, E. C.; Aschmann, S. M., Gas-phase reactions of 1, 4-benzodioxan, 2, 3-dihydrobenzofuran, and 2, 3-benzofuran with OH radicals and O3. *International journal of chemical kinetics* **1992,** *24*, (4), 345-358.

20. Aschmann, S. M.; Arey, J.; Atkinson, R., Rate Constants for the Reactions of OH Radicals with 1,2,4,5-Tetramethylbenzene, Pentamethylbenzene, 2,4,5-Trimethylbenzaldehyde, 2,4,5-Trimethylphenol, and 3-Methyl-3-hexene-2,5-dione and Products of OH + 1,2,4,5-Tetramethylbenzene. *The Journal of Physical Chemistry A* **2013,** *117*, (12), 2556-2568.

21. Magneron, I.; Thevenet, R.; Mellouki, A.; Le Bras, G.; Moortgat, G.; Wirtz, K., A study of the photolysis and OH-initiated oxidation of acrolein and trans-crotonaldehyde. *The Journal of Physical Chemistry A* **2002,** *106*, (11), 2526-2537.

22. Mason, S. A.; Arey, J.; Atkinson, R., Kinetics and Products of the OH Radical-Initiated Reaction of 1,4-Butanediol and Rate Constants for the Reactions of OH Radicals with 4-Hydroxybutanal and 3-Hydroxypropanal. *Environmental Science & Technology* **2010,** *44*, (2), 707-713.

23. Fruekilde, P.; Hjorth, J.; Jensen, N. R.; Kotzias, D.; Larsen, B., Ozonolysis at vegetation surfaces: a source of acetone, 4-oxopentanal, 6-methyl-5-hepten-2-one, and geranyl acetone in the troposphere. *Atmospheric Environment* **1998,** *32*, (11), 1893-1902.

24. Bierbach, A.; Barnes, I.; Becker, K. H.; Wiesen, E., Atmospheric chemistry of unsaturated carbonyls: Butenedial, 4-oxo-2-pentenal, 3-hexene-2, 5-dione, maleic anhydride, 3H-furan-2-one, and 5-methyl-3H-furan-2-one. *Environmental science & technology* **1994,** *28*, (4), 715-729.

25. Davis, M.; Gilles, M.; Ravishankara, A.; Burkholder, J. B., Rate coefficients for the reaction of OH with (E)-2-pentenal,(E)-2-hexenal, and (E)-2-heptenal. *Physical Chemistry Chemical Physics* **2007,** *9*, (18), 2240-2248.

26. Baker, J.; Arey, J.; Atkinson, R., Formation and reaction of hydroxycarbonyls from the reaction of OH radicals with 1, 3-butadiene and isoprene. *Environmental science & technology* **2005,** *39*, (11), 4091-4099.

27. Bierbach, A.; Barnes, I.; Becker, K., Product and kinetic study of the OH-initiated gas-phase oxidation of furan, 2-methylfuran and furanaldehydes at≈ 300 K. *Atmospheric Environment* **1995,** *29*, (19), 2651-2660.

28. Renbaum-Wolff, L.; Smith, G. D., “Virtual Injector” Flow Tube Method for Measuring Relative Rates Kinetics of Gas-Phase and Aerosol Species. *The Journal of Physical Chemistry A* **2012,** *116*, (25), 6664-6674.

29. Grosjean, D.; Williams II, E. L., Environmental persistence of organic compounds estimated from structure-reactivity and linear free-energy relationships. Unsaturated aliphatics. *Atmospheric Environment. Part A. General Topics* **1992,** *26*, (8), 1395-1405.

30. Gao, T.; Andino, J. M.; Rivera, C. C.; Márquez, M. F., Rate constants of the gas-phase reactions of OH radicals with trans-2-hexenal, trans-2-octenal, and trans-2-nonenal. *International Journal of Chemical Kinetics* **2009,** *41*, (7), 483-489.

31. Xing, J.-H.; Ono, M.; Kuroda, A.; Obi, K.; Sato, K.; Imamura, T., Kinetic study of the daytime atmospheric fate of (Z)-3-hexenal. *The Journal of Physical Chemistry A* **2012,** *116*, (33), 8523-8529.

32. Aschmann, S. M.; Arey, J.; Atkinson, R., Atmospheric chemistry of selected hydroxycarbonyls. *The Journal of Physical Chemistry A* **2000,** *104*, (17), 3998-4003.

33. Smith, A. M.; Rigler, E.; Kwok, E. S. C.; Atkinson, R., Kinetics and Products of the Gas-Phase Reactions of 6-Methyl-5-hepten-2-one and trans-Cinnamaldehyde with OH and NO3 Radicals and O3 at 296 ± 2 K. *Environmental Science & Technology* **1996,** *30*, (5), 1781-1785.

34. Baker, J.; Arey, J.; Atkinson, R., Kinetics of the Gas-Phase Reactions of OH Radicals, NO3 Radicals and O3 with Three C7-Carbonyls Formed From The Atmospheric Reactions of Myrcene, Ocimene and Terpinolene. *Journal of Atmospheric Chemistry* **2004,** *48*, (3), 241-260.

35. Albaladejo, J.; Ballesteros, B.; Jiménez, E.; Martín, P.; Martínez, E., A PLP–LIF kinetic study of the atmospheric reactivity of a series of C4–C7 saturated and unsaturated aliphatic aldehydes with OH. *Atmospheric environment* **2002,** *36*, (20), 3231-3239.

36. Tuazon, E. C.; Aschmann, S. M.; Nguyen, M. V.; Atkinson, R., H-atom abstraction from selected C · H bonds in 2, 3-dimethylpentanal, 1, 4-cyclohexadiene, and 1, 3, 5-cycloheptatriene. *International Journal of Chemical Kinetics* **2003,** *35*, (9), 415-426.

37. Atkinson, R.; Aschmann, S. M., Atmospheric chemistry of the monoterpene reaction products nopinone, camphenilone, and 4-acetyl-1-methylcyclohexene. *Journal of atmospheric chemistry* **1993,** *16*, (4), 337-348.

38. Carrasco, N.; Picquet-Varrault, B.; Doussin, J.-F., Kinetic and product study of the gas-phase reaction of sabinaketone with OH radical. *International Journal of Chemical Kinetics* **2007,** *39*, (7), 415-421.

39. Bowman, J. H.; Barket, D. J.; Shepson, P. B., Atmospheric chemistry of nonanal. *Environmental science & technology* **2003,** *37*, (10), 2218-2225.

40. Ceacero-Vega, A. A.; Ballesteros, B.; Bejan, I.; Barnes, I.; Jiménez, E.; Albaladejo, J., Kinetics and mechanisms of the tropospheric reactions of menthol, borneol, fenchol, camphor, and fenchone with hydroxyl radicals (OH) and chlorine atoms (Cl). *The Journal of Physical Chemistry A* **2012,** *116*, (16), 4097-4107.

41. Forester, C. D.; Ham, J. E.; Wells, J., Geraniol (2, 6-dimethyl-2, 6-octadien-8-ol) reactions with ozone and OH radical: Rate constants and gas-phase products. *Atmospheric Environment* **2007,** *41*, (6), 1188-1199.

42. Harrison, J.; Ham, J.; Wells, J., Citronellal reactions with ozone and OH radical: Rate constants and gas-phase products detected using PFBHA derivatization. *Atmospheric Environment* **2007,** *41*, (21), 4482-4491.

43. Atkinson, R., Kinetics and mechanisms of the gas-phase reactions of the hydroxyl radical with organic compounds under atmospheric conditions. *Chemical Reviews* **1986,** *86*, (1), 69-201.

44. Picquet, B.; Heroux, S.; Chebbi, A.; Doussin, J. F.; Durand-Jolibois, R.; Monod, A.; Loirat, H.; Carlier, P., Kinetics of the reactions of OH radicals with some oxygenated volatile organic compounds under simulated atmospheric conditions. *International journal of chemical kinetics* **1998,** *30*, (11), 839-847.

45. Pimentel, A. S.; Tyndall, G. S.; Orlando, J. J.; Hurley, M. D.; Wallington, T. J.; Sulbaek Andersen, M. P.; Marshall, P.; Dibble, T. S., Atmospheric chemistry of isopropyl formate and tert-butyl formate. *International Journal of Chemical Kinetics* **2010,** *42*, (8), 479-498.
46. Bierbach, A.; Barnes, I.; Becker, K., Rate coefficients for the gas-phase reactions of hydroxyl radicals with furan, 2-methylfuran, 2-ethylfuran and 2, 5-dimethylfuran at 300±2 K. *Atmospheric Environment. Part A. General Topics* **1992,** *26*, (5), 813-817.
47. Klotz, B.; Barnes, I.; Becker, K.-H., Kinetic study of the gas-phase photolysis and OH radical reaction of E,Z- and E,E-2,4-Hexadienedial. *International Journal of Chemical Kinetics* **1999,** *31*, (10), 689-697.
48. Ferrari, C.; Roche, A.; Jacob, V.; Foster, P.; Baussand, P., Kinetics of the reaction of OH radicals with a series of esters under simulated conditions at 295 K. *International Journal of Chemical Kinetics* **1996,** *28*, (8), 609-614.
49. Cometto, P. M.; Daële, V.; Idir, M.; Lane, S. I.; Mellouki, A., Reaction Rate Coefficients of OH Radicals and Cl Atoms with Ethyl Propanoate, n-Propyl Propanoate, Methyl 2-Methylpropanoate, and Ethyl n-Butanoate. *The Journal of Physical Chemistry A* **2009,** *113*, (40), 10745-10752.
50. Le Calve, S.; Le Bras, G.; Mellouki, A., Temperature dependence for the rate coefficients of the reactions of the OH radical with a series of formates. *The Journal of Physical Chemistry A* **1997,** *101*, (30), 5489-5493.
51. Szilágyi, I.; Dóbé, S.; Bérces, T.; Márta, F.; Viskolcz, B., Direct kinetic study of reactions of hydroxyl radicals with alkyl formates. *Zeitschrift für Physikalische Chemie* **2004,** *218*, (4), 479-492.
52. Schütze, N.; Zhong, X.; Kirschbaum, S.; Bejan, I.; Barnes, I.; Benter, T., Relative kinetic measurements of rate coefficients for the gas-phase reactions of Cl atoms and OH radicals with a series of methyl alkyl esters. *Atmospheric Environment* **2010,** *44*, (40), 5407-5414.
53. Blanco, M. B.; Taccone, R. A.; Lane, S. I.; Teruel, M. A., On the OH-initiated degradation of methacrylates in the troposphere: Gas-phase kinetics and formation of pyruvates. *Chemical physics letters* **2006,** *429*, (4-6), 389-394.
54. Dagaut, P.; Wallington, T. J.; Liu, R.; Kurylo, M. J., A kinetic investigation of the gas-phase reactions of hydroxyl radicals with cyclic ketones and diones: mechanistic insights. *The Journal of Physical Chemistry* **1988,** *92*, (15), 4375-4377.
55. Holloway, A.-L.; Treacy, J.; Sidebottom, H.; Mellouki, A.; Daële, V.; Le Bras, G.; Barnes, I., Rate coefficients for the reactions of OH radicals with the keto/enol tautomers of 2, 4-pentanedione and 3-methyl-2, 4-pentanedione, allyl alcohol and methyl vinyl ketone using the enols and methyl nitrite as photolytic sources of OH. *Journal of Photochemistry and Photobiology A: Chemistry* **2005,** *176*, (1-3), 183-190.
56. Teruel, M. A.; Benitez-Villalba, J.; Caballero, N.; Blanco, M. B., Gas-Phase oxidation of methyl crotonate and ethyl crotonate. kinetic study of their reactions toward OH radicals and Cl atoms. *The Journal of Physical Chemistry A* **2012,** *116*, (24), 6127-6133.
57. Le Calvé, S.; Le Bras, G.; Mellouki, A., Kinetic studies of OH reactions with Iso-propyl, Iso-butyl, Sec-butyl, and Tert-butyl acetate. *International journal of chemical kinetics* **1997,** *29*, (9), 683-688.
58. Veillerot, M.; Foster, P.; Guillermo, R.; Galloo, J. C., Gas-phase reaction of n-butyl acetate with the hydroxyl radical under simulated tropospheric conditions: Relative rate constant and product study. *International Journal of Chemical Kinetics* **1996,** *28*, (4), 235-243.
59. Stemmler, K.; Mengon, W.; Alistair Kerr, J., Hydroxyl-radical-initiated oxidation of isobutyl isopropyl ether under laboratory conditions related to the troposphere Product studies and

proposed mechanism. *Journal of the Chemical Society, Faraday Transactions* **1997,** *93*, (16), 2865-2875.

60. Blanco, M. B.; Bejan, I.; Barnes, I.; Wiesen, P.; Teruel, M. A., OH-Initiated Degradation of Unsaturated Esters in the Atmosphere: Kinetics in the Temperature Range of 287−313 K. *The Journal of Physical Chemistry A* **2009,** *113*, (20), 5958-5965.

61. Williams, D. C.; O'Rji, L. N.; Stone, D. A., Kinetics of the reactions of OH radicals with selected acetates and other esters under simulated atmospheric conditions. *International Journal of Chemical Kinetics* **1993,** *25*, (7), 539-548.

62. Nizamov, B.; Dagdigian, P. J., Spectroscopic and kinetic investigation of methylene amidogen by cavity ring-down spectroscopy. *The Journal of Physical Chemistry A* **2003,** *107*, (13), 2256-2263.

63. Borduas, N.; da Silva, G.; Murphy, J. G.; Abbatt, J. P. D., Experimental and Theoretical Understanding of the Gas Phase Oxidation of Atmospheric Amides with OH Radicals: Kinetics, Products, and Mechanisms. *The Journal of Physical Chemistry A* **2015,** *119*, (19), 4298-4308.

64. Sun, J.; Tang, Y.; Sun, H.; Pan, Y.; Jia, X.; Pan, X.; Wang, R., Mechanistic and kinetic study of the OH+ C2H5CN reaction. *Chemical Physics Letters* **2008,** *463*, (4-6), 315-321.

65. Nielsen, O. J.; Jørgensen, O.; Donlon, M.; Sidebottom, H. W.; O'Farrell, D. J.; Treacy, J., Rate constants for the gas-phase reactions of OH radicals with nitroethene, 3-nitropropene and 1-nitrocyclohexene at 298 K and 1 atm. *Chemical physics letters* **1990,** *168*, (3-4), 319-323.

66. Barnes, I.; Bastian, V.; Becker, K.; Fink, E.; Nelsen, W., Oxidation of sulphur compounds in the atmosphere: I. Rate constants of OH radical reactions with sulphur dioxide, hydrogen sulphide, aliphatic thiols and thiophenol. *Journal of atmospheric chemistry* **1986,** *4*, (4), 445-466.

67. Falbe-Hansen, H.; Sørensen, S.; Jensen, N.; Pedersen, T.; Hjorth, J., Atmospheric gas-phase reactions of dimethylsulphoxide and dimethylsulphone with OH and NO3 radicals, Cl atoms and ozone. *Atmospheric Environment* **2000,** *34*, (10), 1543-1551.

68. Lindinger, W.; Hansel, A.; Jordan, A., On-line monitoring of volatile organic compounds at pptv levels by means of proton-transfer-reaction mass spectrometry (PTR-MS) medical applications, food control and environmental research. *International Journal of Mass Spectrometry and Ion Processes* **1998,** *173*, (3), 191-241.

69. Amelynck, C.; Schoon, N.; Kuppens, T.; Bultinck, P.; Arijs, E., A selected ion flow tube study of the reactions of H3O+, NO+ and O2+ with some oxygenated biogenic volatile organic compounds. *International Journal of Mass Spectrometry* **2005,** *247*, (1-3), 1-9.

70. Price, D. J.; Day, D. A.; Pagonis, D.; Stark, H.; Algrim, L. B.; Handschy, A. V.; Liu, S.; Krechmer, J. E.; Miller, S. L.; Hunter, J. F.; de Gouw, J. A.; Ziemann, P. J.; Jimenez, J. L., Budgets of Organic Carbon Composition and Oxidation in Indoor Air. Environ Sci Technol 2019, 53, (22), 13053-13063.

71. Tang, X.; Misztal, P. K.; Nazaroff, W. W.; Goldstein, A. H., Volatile Organic Compound Emissions from Humans Indoors. Environ Sci Technol 2016, 50, (23), 12686-12694.

72. Stonner, C.; Edtbauer, A.; Williams, J., Real-world volatile organic compound emission rates from seated adults and children for use in indoor air studies. Indoor Air 2017, 28, (1), 164-172.

73. St Clair, J. M.; Rivera-Rios, J. C.; Crounse, J. D.; Praske, E.; Kim, M. J.; Wolfe, G. M.; Keutsch, F. N.; Wennberg, P. O.; Hanisco, T. F., Investigation of a potential HCHO measurement artifact from ISOPOOH. *Atmos Meas Tech* **2016,** *9*, (9), 4561-4568.

74. Wennberg, P. O.; Bates, K. H.; Crounse, J. D.; Dodson, L. G.; McVay, R. C.; Mertens, L. A.; Nguyen, T. B.; Praske, E.; Schwantes, R. H.; Smarte, M. D.; St Clair, J. M.; Teng, A. P.; Zhang,

X.; Seinfeld, J. H., Gas-Phase Reactions of Isoprene and Its Major Oxidation Products. *Chem Rev* **2018,** *118*, (7), 3337-3390.

75. St. Clair, J. M.; Rivera-Rios, J. C.; Crounse, J. D.; Knap, H. C.; Bates, K. H.; Teng, A. P.; Jørgensen, S.; Kjaergaard, H. G.; Keutsch, F. N.; Wennberg, P. O., Kinetics and Products of the Reaction of the First-Generation Isoprene Hydroxy Hydroperoxide (ISOPOOH) with OH. *The Journal of Physical Chemistry A* **2016,** *120*, (9), 1441-1451.